The Plant Cell, Vol. 9, 1559–1572, September 1997

Two Distinct Sources of Elicited Reactive Oxygen Species in Tobacco Epidermal Cells

Andrew C. Allan and Robert Fluhr[1]

Department of Plant Genetics, Weizmann Institute of Science, P.O. Box 26, Rehovot 76100, Israel

Reactive oxygen species (ROS) play a prominent role in early and later stages of the plant pathogenesis response, putatively acting as both cellular signaling molecules and direct antipathogen agents. A single-cell assay, based on the fluorescent probe dichlorofluorescein, was used to scrutinize the generation and movement of ROS in tobacco epidermal tissue. ROS, generated within cells, quickly moved apoplastically as H_2O_2 into neighboring cells. Two classes of rapidly elicited intracellular ROS, originating from distinct sources, were distinguished. Cryptogein, the fungal elicitor from *Phytophthora cryptogea*, induced ROS from a flavin-containing oxidase source. ROS accumulation could be inhibited by a number of pharmacological agents, suggesting induction through an active signal transduction pathway. The insensitivity of the increase in ROS to the external addition of enzymes that dissipate ROS suggests that this oxidative increase is primarily intracellular. In contrast, amines and polyamines, compounds that form during wounding and pathogenesis, induced ROS at an apoplastic site from peroxidase- or amine oxidase–type enzyme(s). Salicylic acid, a putative inhibitor of cellular catalases and peroxidases, did not induce cellular ROS, as measured by dichlorofluorescein fluorescence. The physiological relevance of ROS-generated signals was indicated by the rapid alteration of the epidermal cell glutathione pool and the cellular redox state. In addition, induction of ROS by all elicitors was correlated with subsequent cell death.

INTRODUCTION

Pathogen-induced oxidative bursts are harnessed by the plant cell both as a means of "poisoning" an invading pathogen and as an intracellular and intercellular messenger of this invasion. Reactive oxygen species (ROS), including hydrogen peroxide (H_2O_2) and superoxide (O_2^-), are the agents of this burst (reviewed in Sutherland, 1991; Mehdy, 1994; Baker and Orlandi, 1995; Bowell et al., 1995; Inzé and Van Montagu, 1995). Although moderately reactive themselves, much of the cellular damage caused by H_2O_2 and O_2^- is the result of conversion to even more reactive species; for example, H_2O_2 is converted in the presence of Fe^{2+} to the extremely toxic hydroxyl free radical (OH·) via the Fenton reaction. However, it is H_2O_2 that is the most attractive candidate for signaling via ROS because of its relatively long life and high permeability across membranes.

Several enzymatic sources of ROS appear to exist in the plant cell. Evidence is accumulating for the activity of a plasma membrane NAD(P)H oxidase analogous to the mammalian enzyme producing O_2^-. Production of ROS during pathogen response can be prevented by diphenyleneiodonium (DPI), an inhibitor of flavin-containing oxidases, including NAD(P)H oxidase (Levine et al., 1994) and xanthine oxidase (Doussiére and Vignais, 1992). Components of a putative plant NAD(P)H oxidase have been identified (Desikan et al., 1996; Groom et al., 1996; Murphy and Auh, 1996). Another source of ROS, elicited during pathogen attack, is a cell wall–located peroxidase. Although peroxidases usually function to dissipate H_2O_2, it appears that fast production of H_2O_2 from this enzyme occurs during alkalization of the apoplast (Bowell et al., 1995), which has been shown to accompany pathogen recognition (Viard et al., 1994; Salzer et al., 1996). It is postulated that cell wall peroxidase functions to cross-link walls and toxify the apoplast. Whether one or more of these systems produce the oxidative burst has yet to be determined; it is possible that they operate in tandem or have different kinetics. For example, Otte and Barz (1996) have recently suggested that ROS produced by NAD(P)H oxidase drives peroxidase-catalyzed oxidative processes. An additional source of ROS may emanate intracellularly from xanthine or aldehyde oxidase activity, as seen in mammalian systems (Hille and Massey, 1985). The molecular characterization of plant xanthine/aldehyde oxidase has been described recently (Ori et al., 1997).

A wide range of factors appears to elicit an oxidative response in plant cells. Abiotic inputs, such as UV-B (280 to 320 nm), temperature extremes, pollutants, and osmotic and mechanical stress, all appear to produce increases in ROS (Green and Fluhr, 1995; Inzé and Van Montagu, 1995; Yahraus et al., 1995). Pathogen-related ROS elicitors mainly include

[1]To whom correspondence should be addressed. E-mail lpfluhr@wiccmail.weizmann.ac.il; fax 972-8-9344181.

pathogen-derived macromolecules that appear to bind plant receptors to induce ROS (Chandra et al., 1996; Scofield et al., 1996; Tang et al., 1996). Two phases of ROS induction by fungal or bacterial elicitors have been measured in plant cell suspension cultures. Very rapid responses (within minutes) have been termed phase I (Baker and Orlandi, 1995) and have been shown to be specifically inhibited by DPI, calcium influx inhibitors, and kinase inhibitors (Baker and Orlandi, 1995; Hammond-Kosack and Jones, 1996). Although phase I production of ROS appears to involve an elicitor–receptor interaction, the responses are not always correlated with plant disease resistance. Later ROS production (many hours) is termed phase II and correlates with the resistance or susceptibility of the plant to the pathogen. Phase I and II bursts differ kinetically; however, they may also differ as to the source of ROS and/or the type of ROS produced.

Previous studies on the oxidative burst have concentrated on the rapid sampling of extracellular ROS produced by cell suspensions. In this study, we used the oxidatively sensitive fluorophore dichlorofluorescein (DCF) to directly measure fast intracellular increases in ROS. In addition to cellular loading, the optical properties of DCF make it amenable to imaging by laser scanning confocal microscopy of leaf tissue. DCF has been used previously in plant cell cultures to visualize oxidative processes in response to mechanical stress (Yahraus et al., 1995) and long-term accumulation of ROS induced by fungal infection of parsley cells, before the occurrence of cell death (Naton et al., 1996). In this study, we describe the use of DCF to monitor fast oxidative cytosolic responses to a number of known elicitors of plant–pathogen responses. Our study differentiates the intracellular oxidative response to two principal sources of ROS: a cell wall peroxidase–like activity and a flavin-containing oxidase system. These responses are measured in fully differentiated epidermal cells rather than in cell culture, which allows the imaging of ROS transients in single cells and their subsequent movement between cells.

RESULTS

DCF Measures Oxidative Potential in Epidermal Peel Cells

Dichlorofluorescin (DCFH) enters cells in the diacetate form (DCFH-DA). Here, it is hydrolyzed and trapped as DCFH, a nonfluorescent compound. Subsequent oxidation of DCFH by H_2O_2, catalyzed by peroxidases, yields the highly fluorescent DCF (Cathcart et al., 1983). DCFH-DA loads readily into epidermal cells of tobacco, and its optical properties make it amenable to laser scanning confocal microscopic analysis, as shown in Figures 1A to 1C. The initial fluorescent image before elicitation shows oxidized dye accumulating in the chloroplast and nucleus of the guard cell (Figure 1B). The low background rate of oxidation is due in part to the oxidizing environment of the chloroplast and can be enhanced by paraquat treatment or reduced by the photosystem II inhibitor atrazine (data not shown). The addition of exogenous H_2O_2 results in rapid enhancement of fluorescence in most cellular compartments, resulting in a twofold increase in pixel intensity averaged over the entire cell within 5 sec (Figure 1C).

DCFH exhibits selectivity for H_2O_2 over other free radicals (Vowells et al., 1995). It is likely, however, that in vivo, other radical species are quickly converted to H_2O_2 and so react with the probe indirectly. Indeed, fluorometry showed DCF to be sensitive to a number of prooxidants or prooxidant-generating systems in addition to H_2O_2 (Figure 2A). For example, generation of O_2^- outside of the cell, using a xanthine/xanthine oxidase system, resulted in a large cellular fluorescence increase (Figure 2B). Although O_2^- has limited permeability across the plasma membrane, O_2^- can rapidly dismutate to H_2O_2 either spontaneously or in a reaction catalyzed by superoxide dismutase (SOD; Sutherland, 1991). Indeed, the addition of exogenous SOD to the O_2^--generating system enhances the rate of intracellular DCFH oxidation

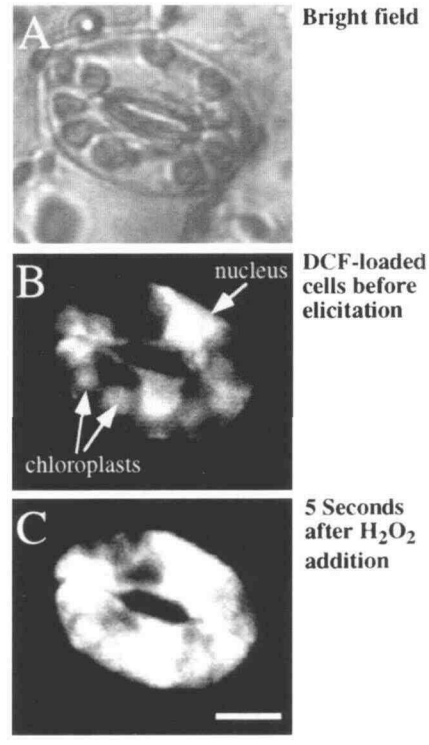

Figure 1. Laser Scanning Confocal Microscopy of H_2O_2-Induced Increases in Intracellular DCF Fluorescence.

Epidermal peels were loaded with DCFH-DA, washed, and examined using a laser scanning confocal microscope.
(A) Bright-field image of a single stomatal complex.
(B) Fluorescence of DCF before stimulation.
(C) Fluorescence 5 sec after the addition of 5 mM H_2O_2.
Bar in **(C)** = 10 μm.

(Figure 2B), whereas catalase abrogates the response (data not shown), indicating that H_2O_2 formed in this manner freely enters the cell. Rose bengal (4,5,6,7-tetrachloro-2′,4′,5′,7′-tetraiodofluoroscein) is a water-soluble xanthene dye that forms singlet oxygen ($^1O_2$) when irradiated with white light (Knox and Dodge, 1984). In the plant, $^1O_2$ is rapidly converted to O_2^- and H_2O_2 (Foyer et al., 1994). Tobacco peel tissue treated with rose bengal showed a rapid light-dependent increase in DCF fluorescence (Figure 2C), suggesting fast conversion of this ROS to H_2O_2. UV-B radiation directly elicits multilevel oxidative processes in plants (Hideg and Vass, 1996) and induces the accumulation of free radical scavenging enzymes (Rao et al., 1996), flavonoids (Li et al., 1993), and pathogenesis-related proteins (Green and Fluhr, 1995). Tissues loaded with DCFH show rapid UV-B–dependent accumulation of fluorescence (Figure 2D). DCFH is not directly oxidized by UV-B because exposure of DCFH in vitro to the same levels of UV-B (5 μmol m^{-2} sec^{-1}) did not induce fluorescence (data not shown).

DCFH oxidation by H_2O_2 requires the presence of peroxidase activity (Cathcart et al., 1983). Thus, intracellular responses of DCFH to exogenously added ROS are limited by the availability of cytosolic peroxidases. This dependency makes the calibration of fluorescent responses to meaningful intracellular H_2O_2 concentrations difficult. However, intracellular DCF fluorescence increases after addition of exogenous concentrations of H_2O_2 from 1 μM to 5 mM (Figure 2E). Thus, within this range of H_2O_2, peroxidase activities are not limiting, and treatments with the other prooxidants and ROS-generating systems (Figure 2E; xanthine/xanthine oxidase, rose bengal, and UV-B) can result in local concentrations of ROS that are equivalent to the addition of micromolar and millimolar amounts of exogenous H_2O_2.

Intercellular ROS Movement Is Apoplastic

H_2O_2 diffusion from elicited tobacco cells activated gene expression in unelicited cells (Levine et al., 1994). We examined the movement of ROS between cells by generating a local ROS signal and examining the response in adjoining cells using the DCF assay. Tissue preloaded with rose bengal and DCFH-DA was exposed to 30 sec of white light precisely focused using the microscope condenser (circled areas; Figures 3A and 3D). Increases in fluorescence were detected during and immediately after white light treatment both in exposed cells and in neighboring cells (Figure 3B). Scanning by using the laser (488 nm excitation) alone was ineffective in inducing measurable activation of rose bengal, and no increase in fluorescence occurred after light exposure in cells loaded with DCFH only (i.e., without rose bengal; data not shown). Changes in the pixel intensity over time in selected cytosolic areas within the exposed cells (area 1), adjacent cells (area 2), and cells not directly adjacent (area 3) are shown in Figure 3C. ROS generated by light exposure quickly traversed to neighboring cells as well as to cells

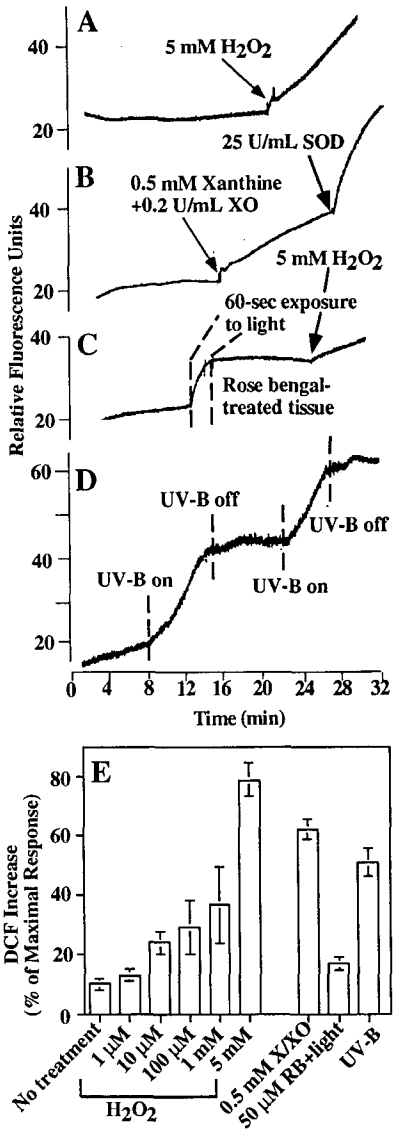

Figure 2. Tissue Fluorescence of DCF in the Presence of Prooxidants.

Epidermal peels were loaded with DCFH-DA, washed, and affixed to a holder in a fluorometer cuvette. Relative fluorescence was monitored during a time course in which in-flight additions of the indicated prooxidants were made.

(A) H_2O_2 (5 mM).

(B) Xanthine oxidase (XO; 0.2 units [U] per mL) and xanthine (0.5 mM), followed by the addition of SOD (25 units per mL).

(C) White light exposure of tissue (70 μmol m^{-2} sec^{-1}) treated with 50 μM rose bengal.

(D) Tissue exposed to a supplementary UV-B light source (5 μmol m^{-2} sec^{-1}).

(E) Mean fluorescence changes over 10 min expressed as a percentage of the maximal response possible, as established by treatment with 5 mM H_2O_2 for 30 min (performed for all fluorometry experiments). The results of three replicate fluorometric experiments (±SE) are shown. RB, rose bengal; X, xanthine; XO, xanthine oxidase.

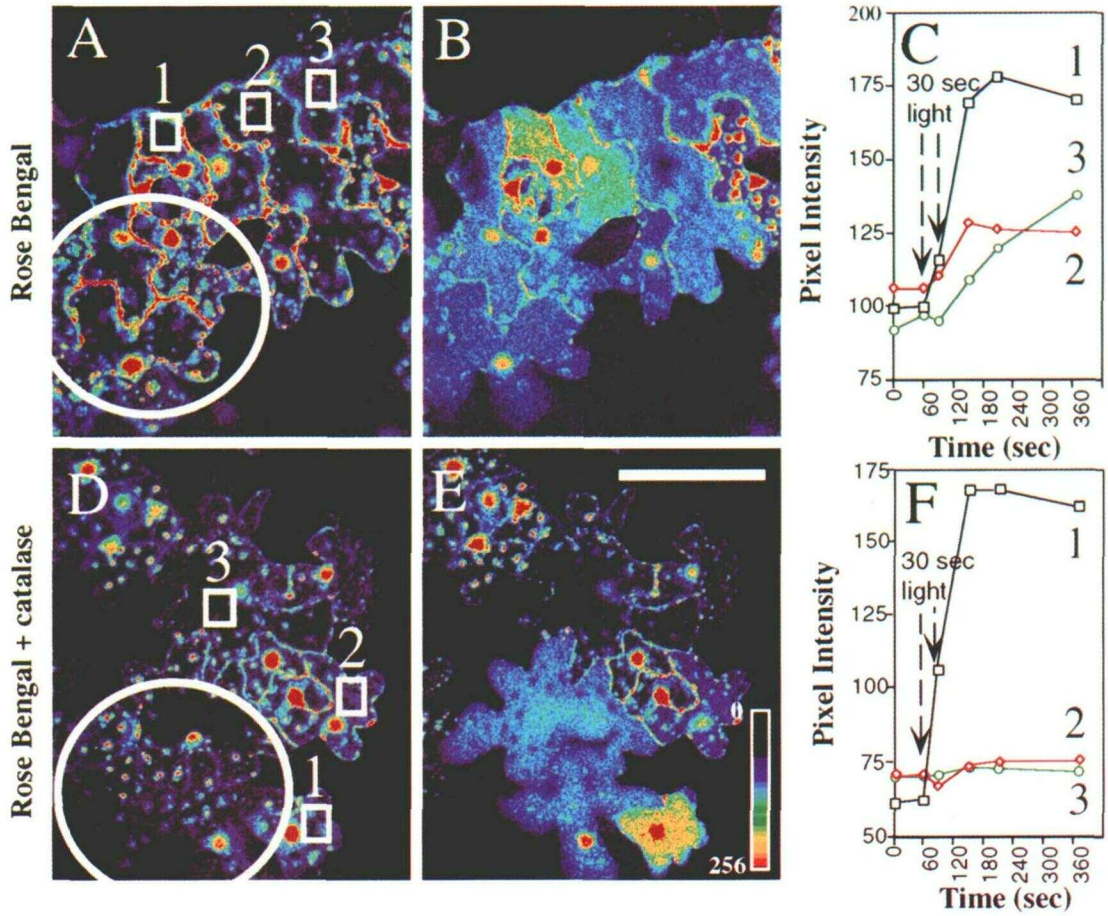

Figure 3. Movement of ROS in Epidermal Tissue.

Epidermal tissue was loaded with DCFH-DA and rose bengal, washed, and examined by laser scanning confocal microscopy. During a time course of image acquisition, bright white light was focused through the microscope condenser on the circled areas, as shown in **(A)** and **(D)**.

(A) DCFH-DA– and rose bengal–treated cells before exposure to light.

(B) Cells shown in **(A)** 180 sec after a white light exposure (30 sec).

(C) Time course of change in pixel intensities of selected cytosolic regions, as represented by the boxes in **(A)**.

(D) DCFH-DA– and rose bengal–loaded cells in the presence of catalase (100 units per mL).

(E) Cells shown in **(D)** 180 sec after a white light exposure (30 sec). The pseudocolor key is shown within the bar, which was applied to pixel intensity values for all of the four fluorescence images.

(F) Time course of change in pixel intensities of selected cytosolic regions as represented by the boxes in **(D)**.

Bar in **(E)** = 80 μm for all images.

without direct symplastic connection (more than one cell away). Little or no increase in ROS was observed in areas that were five or six cells removed from the site of light exposure (up to 15 min after exposure; data not shown), indicating that the generated ROS were dissipated rather than propagated through the tissue.

The addition of catalase before white light exposure abrogated the fluorescence increase in adjacent cells but not in directly exposed cells (Figures 3D to 3F). Because the exogenously added catalase remains in the apoplast, one facet of the induced intercellular movement of ROS apparently involves H_2O_2. Catalase sensitivity rules out the possibility that it is the dye, and not ROS, that is moving between cells. It also indicates that activation of rose bengal by low levels of reflected and/or defracted light outside of the area of focused light exposure was negligible. We suggest that cytosolically generated ROS can leave the cell as H_2O_2 and enter other cells via an apoplastic route, illustrating the potential for H_2O_2 as an intercellular signal. Consistent with this conclusion is the observation that unexposed stomatal guard cells, which have no symplastic connection to their epidermal neighbors, also showed increases in intracellular ROS

when nearby rose bengal–loaded cells were activated to produce ROS (data not shown).

Distinct Sources of Elicitor-Induced Oxidative Bursts

We examined the intracellular accumulation of ROS induced by various types of elicitors. Cryptogein, a small extracellular fungal protein produced by *Phytophthora cryptogea*, induces on its non-host tobacco rapid changes in ion fluxes, the accumulation of ROS, ethylene, and phytoalexins, and finally, hypersensitive cell death (Ricci et al., 1989; Milat et al., 1990; Viard et al., 1994). The application of 25 nM cryptogein to DCFH-loaded tissue resulted in a rapid burst of fluorescence, followed by a steady accumulation of ROS (Figure 4A). This increase in fluorescence was completely inhibited by the antioxidant *N*-acetyl-L-cysteine (at 0.5 mM; see next section).

Salicylic acid (SA) is implicated in systemic pathogen resistance and has been postulated to enhance H_2O_2 accumulation via inhibition of a cytosolic catalase (Chen et al., 1993).

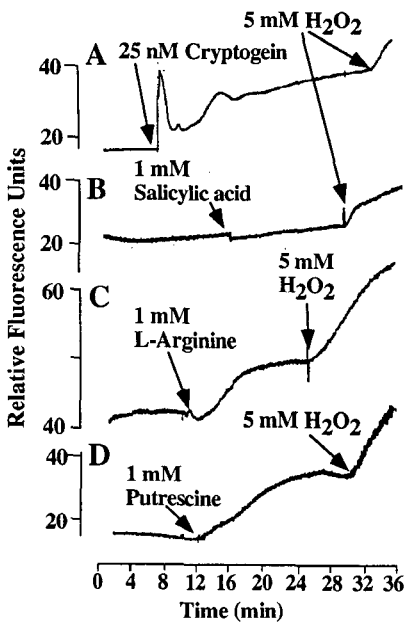

Figure 4. Tissue Fluorescence of DCF in the Presence of Exogenous Elicitors.

Epidermal peels were loaded with DCFH-DA, washed, and affixed to a holder in a fluorometer cuvette. Fluorescence was then monitored during a time course in which in-flight additions were made that were followed by the addition of 5 mM H_2O_2.

(A) Cryptogein (25 nM).

(B) Salicylic acid (1 mM).

(C) L-Arginine (1 mM).

(D) Putrescine (1 mM).

Application of SA to DCFH-loaded tissue caused little or no detectable change in fluorescence (Figure 4B). The tissue's sensitivity to the subsequent addition of exogenous H_2O_2 was slightly reduced, indicating that SA may inhibit peroxidases required for the DCF assay (Figure 4B). Inhibition of ascorbate peroxidase by SA has been observed (Durner and Klessig, 1995). However, it is unlikely that cytosolic peroxidases are inhibited by SA to the extent that DCFH cannot be converted to DCF by SA-generated ROS, because L-arginine continued to stimulate DCFH oxidation when L-arginine and SA were added simultaneously (data not shown).

Another possible source of ROS in plants is the production of nitric oxide (NO). In animal systems, NO synthase uses L-arginine as a substrate to produce NO and L-citrulline. NO synthase activity has recently been demonstrated in plants (Ninnemann and Maier, 1996). Application of NO to DCFH-loaded tissue via the NO donor (±)-*S*-nitroso-*N*-acetylpenicillamine resulted in a large increase in fluorescence (data not shown), indicating that NO or its ROS derivatives were effectively reported by DCF, as shown in human neutrophil cells (Rao et al., 1992). Therefore, we tested whether NO synthase activity could be detected in tobacco cells. Application of L-arginine to the DCFH-loaded cells resulted in a large increase in DCF fluorescence (Figure 4C). This was specific for the L-isomer and was inhibited by the NO synthase inhibitor *N*-monomethyl-L-arginine monoacetate (L-NMMA; see next section). However, other amines produced a similar burst, including L-histidine, L-citrulline, L-glutamine, canavanine, and the polyamines spermidine, spermine, and putrescine (data shown for putrescine; Figure 4D). L-Arginine and putrescine had no in vivo effects on the pH indicators SNARF-1 and fluorescein (data not shown).

Amines can induce ROS production by acting as substrates for amine oxidases. These are a ubiquitous group of plant enzymes that catalyze the oxidation of a variety of monoamines, diamines, and polyamines to the corresponding aldehyde and release NH_3 and H_2O_2 (Tipping and McPherson, 1995). Peroxidase can also produce H_2O_2 when supplied with an appropriate reductant (Bowell et al., 1995). We examined ROS production in vitro with commercially available type I horseradish peroxidase by using the luminol assay and readily detected a catalase-sensitive ROS increase with L-arginine and putrescine (data not shown). This ROS production shows both L-isomer selectivity and inhibition by L-NMMA similar to that detected in vivo with tobacco tissue. These observations are consistent with the amine oxidase activity associated with peroxidase.

Catalase Sensitivity Differentiates Responses into Two Classes

Fluorometric experiments performed with epidermal cells, using the elicitors of oxidative bursts, in the presence or absence of catalase, distinguished two types of response. Bursts induced by L-arginine and putrescine were highly

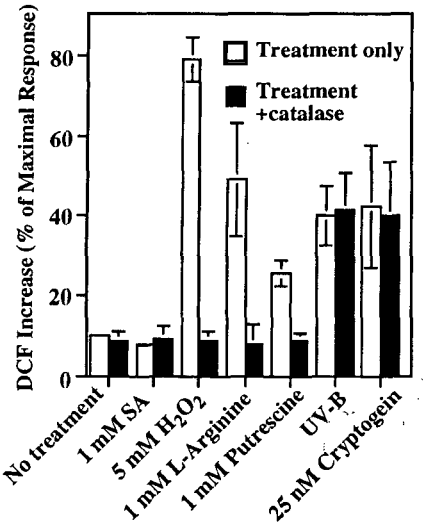

Figure 5. Elicitor-Induced DCF Increases in the Presence or Absence of Catalase.

Fluorometric experiments were performed as described in the legend to Figure 4. The mean rate of increase of the elicited response, during a 10-min duration, is expressed as a percentage of the maximal response obtained after the addition of H_2O_2. Experiments were performed in the presence or absence of catalase (100 units per mL). The results of three replicate experiments are shown (±SE).

sensitive to catalase (100 units per mL; Figure 5), as was the addition of exogenous H_2O_2. The second class of elicitor showed no catalase sensitivity at these concentrations and included cryptogein and UV-B. A possible explanation for the observed differential sensitivities to catalase is that the amine class of elicitor causes an apoplastic extracellular increase in H_2O_2 (which subsequently enters the cell), whereas cryptogein and UV-B result in cytosolic production of ROS. Alternatively, cryptogein may increase apoplastic levels of a catalase-insensitive radical such as O_2^-, which protonates to HO_2^- to enter the cell and so react with the intracellular DCFH probe. However, neither cryptogein- nor L-arginine–induced intracellular ROS, monitored by DCF fluorescence, showed sensitivity to SOD (data not shown).

Imaging of DCF fluorescence by laser scanning confocal microscopy was used to further distinguish between the two classes of elicited burst. Both elicitor types appeared to induce fast cytosolic bursts in reactive oxygen (Figures 6A to 6D). As with fluorometry, imaging in the presence of catalase revealed that increases in fluorescence induced by L-arginine were catalase sensitive, whereas cryptogein elicitation was not (data not shown). To determine which cellular compartments had undergone increases in fluorescence, subcellular regions were delineated using bright-field analysis. Peripheral regions were defined as the area including and adjacent to the cell wall, whereas the cytosol was the region devoid of visible organelles, possibly including cytoplasmic and vacuolar regions. Quantitative analysis of pixel intensity was performed over time in peripheral, cytosolic, choroplastic, and nuclear regions, as shown in Figure 6E. A rapid and continuous increase in fluorescence was observed in all cell regions after elicitation with L-arginine and is prominent at the periphery (Figures 6D and 6E). In cryptogein-elicited cells, little or no peripheral increase in fluorescence occurred (Figures 6B and 6E). The earliest increases in cryptogein-induced ROS were in the chloroplastic and nuclear regions; these increases occurred within the first 30 to 60 sec, with the cytosol showing the most sustained increases. Because DCF is a single-wavelength probe, no adjustment can be made for differential loading and redistribution between compartments during experimentation (e.g., reloading into the vacuole). However, the two elicitors appear to produce different recorded responses suggestive of distinct spatial origins of ROS during induction by either cryptogein or L-arginine.

The two sources of elicited ROS could be further differentiated by the application of pharmacological agents. Both classes of burst were completely inhibited by the antioxidant *N*-acetyl-L-cysteine (Figure 7). L-Arginine–induced ROS was sensitive to the NO synthase inhibitor L-NMMA, whereas the burst induced by cryptogein was insensitive to this inhibitor (Figure 7). Cryptogein, however, displays sensitivity to a number of inhibitors of plant signal transduction pathways. The ROS burst showed a high sensitivity to the phosphatase 2A inhibitor okadaic acid and the inhibitor of protein kinase C, staurosporine, whereas the L-arginine–induced burst remained unaffected by both agents (Figure 7). DPI is an inhibitor of flavin-containing oxidases, which includes NAD(P)H oxidase and xanthine oxidase, and has been shown to inhibit several elicited ROS bursts in plants (Levine et al., 1994; Jabs et al., 1996; Otte and Barz, 1996). Cryptogein-induced ROS was significantly inhibited by DPI, whereas the L-arginine–induced burst remained unaffected. Interestingly, induction of ROS by UV-B was also DPI sensitive (data not shown). The use of this range of inhibitors suggests that signal transduction pathways are invoked by cryptogein to produce the early ROS response from a putative NAD(P)H oxidase–type enzyme or another flavin-containing oxidase such as xanthine oxidase. The lack of fluorescence changes in the periphery of imaged cells upon elicitation with cryptogein, as well as an insensitivity to catalase and SOD, suggests that this oxidase is located internal to the plasma membrane. Amines appear to act as substrates for cell wall–located enzymes.

ROS Increases Correlate with Altered Cellular Redox State

If rapid increases in cytosolic ROS (as reported by DCFH oxidation) are physiologically relevant, then they should be accompanied by changes in the redox state of the cell. GSH is a tripeptide thiol that acts as the cell's thiol antioxidant.

Oxidation of GSH results in a disulfide bond linking two molecules of GSH (termed GSSG), which is maintained at low concentrations in the cell by the action of glutathione reductase. The relatively high concentrations of GSH in the cell act to ensure stable maintenance of the cellular thiol state. The state of the cell's GSH/GSSG pool is therefore a very useful endogenous indicator of the occurrence of oxidative stress. If levels of ROS rise in the cell, then the GSH/GSSG ratio is expected to fall due to the action of the enzyme GSH peroxidase, which converts GSH and H_2O_2 to GSSG and H_2O. Therefore, we tested whether elicited ROS bursts resulted in changes in the epidermal cell GSH pool. The application of cryptogein and L-arginine to epidermal peels resulted in a rapid reduction in the ratio of GSH/GSSG from 6 to 4 within 15 min (Figure 8). This change in ratio involved both a GSH decrease and a GSSG increase. Therefore, it appears that the intracellular redox state of the cell reacts rapidly to the accumulation of ROS induced by either class of elicitor.

Epidermal Cell Death after ROS Elicitation

We determined the long-term effect of elicitors of oxidative bursts on cell viability. After 24 to 48 hr, cells of the epidermis

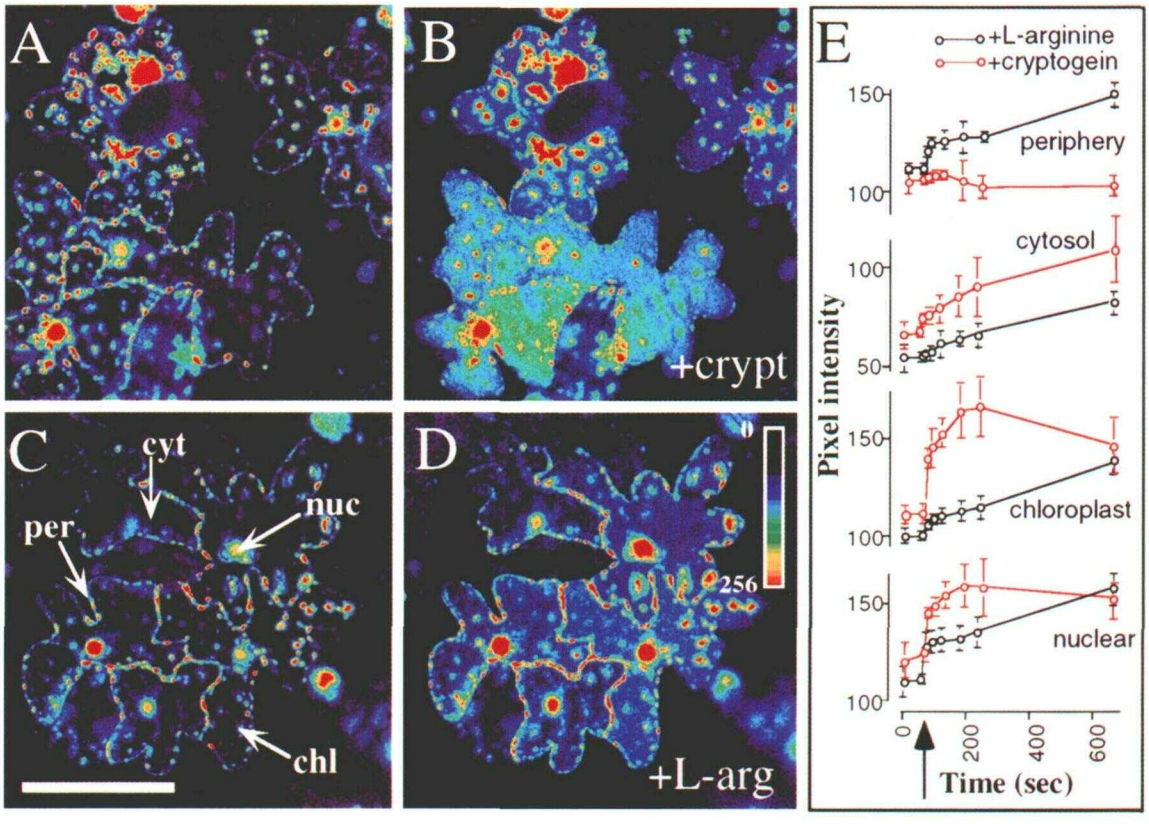

Figure 6. Laser Scanning Confocal Imaging of Elicited Oxidative Bursts in Epidermal Cells.

Epidermal tissue was loaded with DCFH-DA, washed, and examined by laser scanning confocal microscopy. Elicitors were added during the time course of image acquisition.

(A) Epidermal cells loaded with DCFH.

(B) Cells shown in **(A)** 600 sec after the addition of 25 nM cryptogein (+crypt).

(C) Epidermal cells loaded as given in **(A)**. Arrows indicate regions analyzed for changes in pixel intensity. chl, chloroplast; cyt, cytosolic region; nuc, nuclear region; per, periphery of cell.

(D) Cells shown in **(C)** 600 sec after the addition of 1 mM L-arginine (+L-arg). The pseudocolor key is included and was applied to pixel intensity values for all four fluorescence images.

(E) Time course of pixel intensities of selected regions shown in **(C)**. At 60 sec (arrow), 1 mM L-arginine (black circles) or 25 nM cryptogein (red circles) was added. Each time point represents the mean of nine measurements of pixel intensity of each cell compartment determined in three independent experiments (±SE).

Bar in **(C)** = 50 μm for **(A)** to **(D)**.

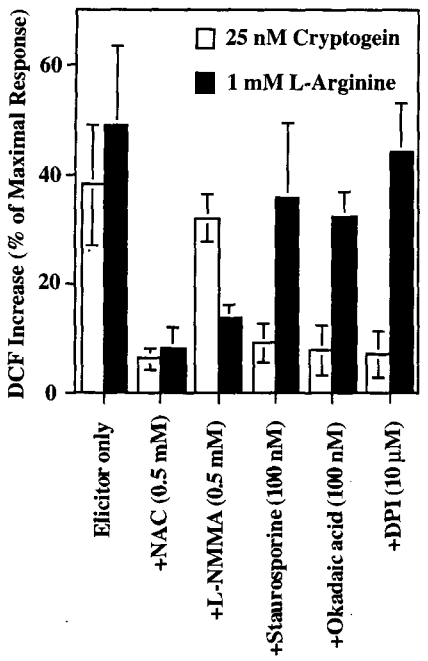

Figure 7. Effect of Pharmacological Agents on Induction of ROS by Cryptogein and L-Arginine.

Increases in DCF fluorescence in tobacco epidermal cells are shown as the percentage of maximal response after the addition of cryptogein (25 nM) or L-arginine (1 mM) in the presence (+) of the indicated pharmacological agents. Results (±SE) are shown for three replicate experiments. NAC, *N*-acetyl-L-cysteine; L-NMMA, *N*-monomethyl-L-arginine monoacetate; DPI, diphenyleneiodonium.

showed good viability (Table 1). However, inclusion of cryptogein, L-arginine, and SA or exposure to UV-B resulted in epidermal cell death (Table 1). Interestingly, guard cells were generally more viable than epidermal cells and were strikingly insensitive to the addition of L-arginine. The addition of catalase to tissues treated with L-arginine or cryptogein had a protective effect, even though the rapid burst induced by cryptogein is catalase insensitive (Figure 5). Production of O_2^- from a xanthine/xanthine oxidase system caused epidermal cell death that could not be prevented by catalase. In addition, guard cells were insensitive to O_2^-. SA (500 μM) causes death of all cell types by 48 hr, even though similar concentrations do not result in short-term changes in oxidative potential (Figures 4 and 5). The cell death promoted by SA cannot be prevented by catalase. Thus, elicitation of ROS is associated with subsequent cell death; however, there are other pathways implicated in plant pathogen response that do not appear to invoke ROS but nevertheless result in cell death.

DISCUSSION

Source of Intracellular ROS

The development of technologies for precise ROS measurement will further our understanding of stress-related oxidative responses during plant photosynthetic and pathogenic processes. The chemical properties of the probe DCFH-DA, coupled with laser scanning confocal microscopy and fluorometric quantification, can be one such tool if the relevant caveats are kept in mind. DCFH preferably uses H_2O_2 in a peroxidase-based activation (Vowells et al., 1995). However, the ultimate formation of H_2O_2 from various species of reactive oxygen and other free radicals, by both spontaneous and enzyme-catalyzed processes, facilitates DCFH reporting of increases in O_2^-, $^1O_2$, and NO. The discrimination of which primary species are induced during bursts invoked by biotic elicitors is then based on differential sensitivity to externally applied agents. The catalase sensitivity of amine-elicited cytosolic ROS suggests that amines induce H_2O_2 influx into the cell after generation in the apoplast. In contrast, the other class of ROS elicitors, typified by cryptogein and UV-B, was insensitive to extracellular catalase and SOD. A comparison using confocal imaging of ROS induction by the two classes of elicitor supports different localization of amine- and cryptogein-induced ROS. The peripheral increases in DCF fluorescence, which were readily observed with L-argi-

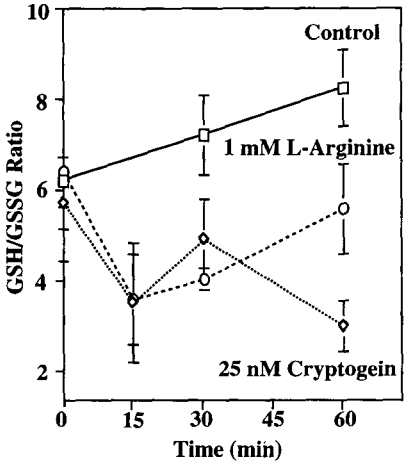

Figure 8. Effect of Elicitor Addition on the Reduced-to-Oxidized GSH Ratio in Epidermal Peel Tissue.

Epidermal peels were floated on sucrose-containing loading buffer, and cryptogein (25 nM) or L-arginine (1 mM) was added. Samples of peel tissue were removed at the indicated time points, and an analysis of glutathione content was made. Each time point represents the mean (±SE) of three separate experiments.

Table 1. Viability of Epidermal Tissue after Exposure to Elicitors, Prooxidants, or Prooxidant Generators

Treatment[a]	Epidermal Cells	Guard Cells	Epidermal Cells (+Catalase)[b]	Guard Cells (+Catalase)[b]
Control	64 ± 5[c]	92 ± 10	72 ± 5	90 ± 12
Cryptogein (25 nM)	3 ± 0	5 ± 0	81 ± 9	92 ± 3
L-Arginine (1 mM)	5 ± 4	93 ± 10	30 ± 11	95 ± 10
SA (500 μM)	0	5 ± 5	0	12 ± 4
UV-B (3 μmol m^{-2} sec^{-1})	0 ± 0	5 ± 2	0 ± 0	9 ± 5
H_2O_2 (5 mM)	0 ± 0	0 ± 0	42 ± 13	89 ± 8
Xanthine oxidase (0.2 units per mL) and xanthine (0.5 mM)	8 ± 2	95 ± 6	5 ± 8	95 ± 4

[a]Epidermal peels were floated on sucrose-supplemented loading buffer to which the indicated treatments were made. After 48 hr (or 24 hr in the case of UV-B–treated tissue only), peels were removed and loaded with fluorescein diacetate, and viability was scored.

[b]Catalase was added at the beginning of the experiment (100 units per mL).

[c]Numbers are the percentage of total cells counted. At least 100 cells were counted for each treatment, and the experiments were repeated in triplicate.

nine, were not observed after cryptogein elicitation. The apparent source for cryptogein-induced ROS is the putative NAD(P)H oxidase system or perhaps an intracellular flavin-containing oxidase, such as xanthine oxidase. The lack of sensitivity to SOD/catalase indicates that ROS is first produced within the cell or in an external position that is inaccessible to ROS-dissipative agents.

To date, most measurements of ROS have used extracellular ROS-sensitive probes. An external O_2^- ROS signal has been hypothesized. This hypothesis is based on stimulation by SOD of elicited bursts (Schwacke and Hager, 1992; Vera-Estrella et al., 1992; Desikan et al., 1996; Doke et al., 1996). However, other reports show that elicited extracellular ROS is not affected by SOD (Apostol et al., 1989; Levine et al., 1994). Interestingly, in this respect, in the mammalian NAD(P)H oxidase system (upon which the plant model is based), the release of ROS occurs only after internalization of the elicitor by phagocytosis (Segal and Abo, 1993). After phagocytosis, the O_2^- radical remains internalized, making H_2O_2 the only likely ROS to leave the cell.

A range of concentrations of SA was ineffective at stimulating increases in intracellular ROS, as determined by the use of DCF. However, Chen et al. (1993) showed significant accumulation of H_2O_2 in tobacco leaves within 3 hr of treatment with 1 mM SA. This discrepancy may be due to the fact that epidermal cells differ, in this respect, from the whole-leaf tissue or that SA invokes H_2O_2 with slow kinetics not amenable to determination by the use of DCF. Alternatively, as has recently been suggested, SA may not induce significant cytosolic changes in H_2O_2 (Bi et al., 1995; Neuenschwander et al., 1995).

Physiological Significance of Extracellular ROS

The kinetics and inhibitor specificity of the L-arginine/polyamine response are suggestive of a largely unregulated substrate-induced burst, and it remains to be determined whether this system has physiological significance during the course of pathogenesis. Amine oxidases, which catalyze the conversion of biogenic amines to aldehyde, ammonia, and H_2O_2, are located in the extracellular space (Agró and Rossi, 1992; Tipping and McPherson, 1995) and are candidates for generating this H_2O_2. Alternatively, apoplastic alkalization, associated with the very early reaction between pathogen elicitors (including cryptogein) and plant cells (e.g., Bottin et al., 1994; May et al., 1996), can induce the activity of cell wall–located peroxidases to produce H_2O_2 (Bowell et al., 1995). Generation of H_2O_2 from extracellular amine oxidases and/or peroxidases, however, necessitates a sustained source of substrate. Our experiments using L-arginine and other amines/polyamines suggest one such source. During pathogen invasion, the apoplast pH rises, favoring an H_2O_2 burst, and electrolyte leakage (shown to accompany cryptogein elicitation of tobacco cells; Bottin et al., 1994) would include many likely substrates for peroxidase and/or amine oxidase to produce sustained H_2O_2 production. In this context, many plants are induced to accumulate higher levels of polyamines and amine-oxidizing systems during pathogen infection, and this positively correlates with resistance (Angelini et al., 1993).

Intercellular movement of pathogen-induced H_2O_2 has been observed by using two populations of soybean suspension cultures separated by a dialysis membrane (Levine et al., 1994). In our study, movement of ROS between cells of the epidermis was observed by following the redistribution of rose bengal–induced ROS. Imaging ROS movement in tissue showed it to be apoplastic, sensitive to catalase, and dissipative in nature. This perhaps reflects a number of antioxidant mechanisms existing in the apoplast, including catalases. Long-distance signaling induced by H_2O_2 is therefore likely to occur only if reiterative factors are present or dissipative agents are modified. For example, spreading hypersensitive lesions induced by pathogens and O_2^- only occur in mutants of Arabidopsis; wild-type plants show only localized lesions (Jabs et al., 1996).

Regulation of ROS by Signal Transduction Pathways

The two sources of ROS appear to be distinct in both their location and sensitivity to pharmacological agents. Only the catalase-insensitive burst induced by cryptogein and UV-B showed sensitivity to inhibitors of plant signal transduction. The sensitivity of the cryptogein response to the protein kinase C inhibitor staurosporine has been shown (Viard et al., 1994). Cryptogein-induced ROS also shows a high sensitivity to the phosphatase 2A inhibitor okadaic acid. This compound inhibits phagocytotic induction of NAD(P)H oxidase by phorbol myristate acetate (Segal and Abo, 1993), a compound recently shown to induce ROS from Arabidopsis protoplasts (Desikan et al., 1996). Previous studies have implicated NAD(P)H oxidase activity during bursts elicited by pathogen-derived macromolecules by showing sensitivity to DPI (Levine et al., 1994; Jabs et al., 1996; Otte and Barz, 1996). However, the mammalian xanthine oxidase also shows sensitivity to DPI (Doussiére and Vignais, 1992). Taken together with evidence for rapid cryptogein-induced changes in ion flux (Viard et al., 1994) and calcium influx (Tavernier et al., 1995), these results suggest that cryptogein invokes a very rapid and complex signal transduction pathway leading to ROS production from a flavin-containing oxidase, such as NAD(P)H oxidase or xanthine oxidase. The temporal sequence of these events should be amenable to simultaneous imaging of calcium and ROS transients.

UV-B radiation induces ROS intracellularly, and its effects are inhibited by DPI. This indicates that UV-B may be stimulating processes that induce an NAD(P)H oxidase or flavin oxidase activity as well as having direct ionizing effects (Hideg and Vass, 1996). UV-B has been shown to induce pathogen responses in tobacco by using signal transduction pathways similar to elicitor-induced responses (Green and Fluhr, 1995). In mammalian systems, UV light rapidly (5 min) invokes kinase activity (Devary et al., 1992) via increases in ROS (Huang et al., 1996). To our knowledge, however, induction of flavin-containing oxidases has not been implicated.

ROS as a Message for Cellular Response

The DCF-based fluorescence assay portrays the potential of ROS as a rapid, all-pervasive signal within the plant cell. The accompanying swift adjustment of the cell's redox state, as determined by the GSH/GSSG ratio, suggests a direct role for ROS as an intracellular message. Changes in the GSH/GSSG ratio have also been observed during the treatment of tomato cells with race-specific elicitors of *Cladosporium fulvum* (May et al., 1996).

In mammalian cells, stress transcription factors, such as nuclear factor-κB and activator protein-1, are redox regulated (Schreck et al., 1992; Meyer et al., 1993; Sen and Packer, 1996). Indeed, epidermal growth factor stimulation of tyrosine phosphorylation in carcinoma cells was shown to be mediated by cytosolic production of H_2O_2 (Bae et al., 1997). In plants, gene activation by ROS was shown during the rapid induction of pathogenesis-related (PR) proteins, which was abrogated by ROS scavengers (Green and Fluhr, 1995). Suppression of catalase activity in tobacco under high light intensity (Chamnongpol et al., 1996), or direct application of H_2O_2 (Bi et al., 1995), also results in PR protein induction, suggesting H_2O_2 as an upstream messenger for redox regulation of PR genes. A tobacco Myb1 oncoprotein homolog, induced within 15 min of SA treatment, has been shown to specifically bind the promoter of PR-1, suggesting the intriguing possibility that this early interaction is redox sensitive because of the presence of a redox-sensitive cysteine in Myb1 (Yang and Klessig, 1996). Direct redox regulation by prooxidants of sensitive cysteine sulfhydryl groups in zinc finger DNA binding proteins may serve to modulate gene expression (Wu et al., 1996). In addition, a zinc finger–containing protein mediates an O_2^--initiated programmed cell death response in Arabidopsis (Dietrich et al., 1997). In this respect, the relatively high elicited ROS levels detected around the nucleus may be relevant.

Post-transcriptional and respiratory processes, such as mitochondrial phosphorylation events (Håkansson and Allen, 1995) and initiation of translation in the chloroplast (Danon and Mayfield, 1994), have also been shown to be redox regulated. This can be via direct effects on protein thiol state, changing the activity of key enzymes. The ubiquity of potential redox-sensitive systems, which includes such varied responses as sensing light–dark transitions, high irradiance stress, and pathogen response, raises the question of how specificity is achieved. The presence or induction of specific dissipative agents suggests one mechanism.

ROS and Cell Death

Elicitors of ROS described in this study hastened cell death, which could be abated by the presence of catalase, except in the case of UV-B. SA did not induce changes in ROS at concentrations that were very effective in causing cell death. SA-induced cell death was not attenuated by catalase, indicating that alternative pathways are initiated by these elicitors of plant pathogenesis. In whole tissues, millimolar application of SA generally does not cause cell death (e.g., 1 mM; Chen et al., 1993). The enhanced sensitivity of the epidermis may be due to an absence of SA secondary metabolism or additional signals emanating from wounding in combination with SA. It is therefore possible that the toxicity of SA to these cells has nothing to do with its role in disease resistance.

Guard cells were generally more resistant to cell death induced by O_2^-, H_2O_2, and L-arginine. This may be a result of the abundance of chloroplasts in this cell type and their accompanying ROS detoxification systems, which are an inherent part of the photosynthetic process. The lack of resistance of guard cells to cryptogein-induced death may indicate that their ROS dissipative capacity is overloaded or that additional factors are induced by cryptogein that enhance cell death. In

addition, cryptogein-induced death was catalase sensitive, yet early cryptogein-induced intracellular ROS increases, as measured by using DCF, were catalase insensitive (Figure 5). It is likely that the extracellular dissipation of ROS can prevent the large buildup of H_2O_2 required to drive cell death. The generation of O_2^- by xanthine oxidase promoted cell death, which could not be reversed by catalase, although catalase abrogated xanthine oxidase–induced DCF fluorescence increases. This indicates that the damaging effect is the likely result of O_2^- and not H_2O_2, as has also been shown by Jabs et al. (1996). Moreover, the lethal damage done by O_2^- happens outside of the cell membrane.

The time sequence of DCF-reported reactivity corresponds to early phase I responses between bacterial and plant cells (Baker and Orlandi, 1995). This phase invokes active signal transduction pathways but does not specify resistance or susceptibility to the pathogen. Phase II responses (4 to 8 hr) are associated with subsequent hypersensitive cell death and resistance to the pathogen (Baker and Orlandi, 1995). Characterizing ROS during these two phases will help to delineate the signal transduction pathways of pathogenesis.

METHODS

Chemicals and Treatments

Dichlorofluorescin diacetate (DCFH-DA) (Molecular Probes, Eugene, OR) was dissolved in DMSO to produce 100 mM stock, which was frozen as aliquots. Cryptogein was a kind gift of P. Ricci and H. Keller (INRA, Antibes, France). The signal transduction inhibitors staurosporine, K-252a, mastoparan, and *N*-monomethyl-L-arginine monoacetate (L-NMMA) and the nitric oxide (NO) donor (±)-*S*-nitroso-*N*-acetyl-penicillamine were purchased from Calbiochem (La Jolla, CA), H_2O_2 from Merck (Darmstadt, Germany), and SNARF-1 from Molecular Probes (Eugene, OR). UV-B irradiation was provided by a Rayonet RPR-3000A lamp (Southern New England Ultraviolet Company, Hamden, CT). Horseradish peroxidase (type I; P-8125) and catalase (bovine liver; C-30) were from Sigma. Unless stated otherwise, other chemicals were of analytical grade and were purchased from Sigma.

Laser Scanning Confocal Microscopy and Fluorometry

The first fully expanded leaves were removed from greenhouse-grown tobacco plants (*Nicotiana tabacum* cv Xanthi). Epidermal peels were then removed from the abaxial surface of each leaf and placed into a small Petri dish containing 10 mL of loading buffer (Tris-KCl at 10 and 50 mM, respectively, pH 7.2) and 5 μL of DCFH-DA from a 100 mM stock in DMSO. Peels were maintained in the dark for 10 min to obtain low basal levels of reactive oxygen species (ROS). For some experiments, peel tissue was also loaded in the presence of 50 μM rose bengal. The peels were then removed, floated on a dish of fresh buffer to wash off excess dye, and affixed to a glass coverslip with silicon grease (high vacuum, heavy; Merck) on which the peel remained immersed in 0.5 mL of loading buffer. Examination of peels was performed using a Bio-Rad MRC-1024 laser scanning confocal microscope. A green argon–ion laser (488 nm) set on 3% power was used for excitation, with 525 nm emission. The viability of the cells within the epidermis under these media conditions was >95% for guard cells and 80% for epidermal cells, as tested by fluorescein diacetate staining. Images were captured over a time course, with laser scanning at set time points to avoid photoactivation of the dye. Elicitors or enzymes (no greater than a 50-μL volume) were added directly to the buffer during the time course. Analysis of images was performed on a Power Macintosh 7200 computer (Apple Computer, Inc., Cupertino, CA), using the public domain National Institutes of Health image program (National Technical Information Service, Springfield, VA).

For fluorometry of whole tissue, a single peel loaded as described above was placed flat onto a polyacrylate plastic holder and affixed at both ends with silicon grease. The holder was inserted into a 3-mL polyacrylate fluorometer cuvette containing 2 mL of aerated loading buffer. The fluorometer (model LS-5B; Perkin-Elmer, Beaconsfield, UK) was set to an excitation of 488 nm and an emission of 525 nm, with slit widths at 5 nm. The cuvette was then placed into the fluorometer and, after establishing a stable baseline, elicitors, enzymes, or pharmacological agents were added. Exposure to supplementary light (UV-B at 5 μmol m^{-2} sec^{-1} or white light at 70 μmol m^{-2} sec^{-1}) was achieved by using a liquid light guide (Lumatec, Munich, Germany). For statistical purposes, fluorometry experiments were performed in triplicate, and fluorescence increases (over 10 min) were expressed as a percentage of the maximal increase possible from the tissue (determined by exposing the tissue to 5 mM H_2O_2 for 30 min at the end of each experiment).

Luminol-Based Chemiluminescence Assay of H_2O_2

Assays were performed in 80 μL of loading buffer containing 1 mM amino acid or polyamine and 10 μL of a 0.2 mg/mL stock of luminol (dissolved in DMSO) within a well of a Microlite plate (Dynatech Laboratories, Chantilly, VA). Reactions were initiated by the addition of 10 μL of a 20 unit per mL stock of horseradish peroxidase, and luminescence counts were measured in an ML 3000 Microtiter Plate Luminometer (Dynatech Laboratories). Each compound was tested at least in triplicate in the presence or absence of catalase (100 units per mL).

Measurement of GSH and GSSG

Reduced and oxidized glutathione (GSH and GSSG) was measured using a modified method for GSH measurement in microtiter plates (Baker et al., 1990). Briefly, epidermal tissue was peeled and floated on buffers with or without elicitors for the designated time. For each replicate, 20 peels (~100 mg of tissue) were gently blotted, weighed, and then immediately frozen in liquid N_2. The tissue was homogenized in 300 μL of 5% sulfosalicylic acid, the homogenate was centrifuged at 15,000*g* for 10 min, and the supernatant was divided into two aliquots. 2-Vinylpyridine (0.35 M final) was added to one aliquot to conjugate GSH, neutralized to pH 6.5 with triethanolamine (10 μL), and allowed to stand at room temperature for 30 min. Oxidized glutathione concentrations in these neutralized extracts were determined using the enzymatic recycling assay (Baker et al., 1990) involving the color development at 412 nm of 5,5-dithiobis 2-nitro-benzoic acid in the presence of NADPH (0.25 mM) and GSH reductase (1.25 units per mL). Total GSH plus GSSG levels were determined using the

same assay from aliquots without added 2-vinylpyridine. GSH standards treated in the same way were used to calibrate the assay.

Cell Viability Assay

Peels were floated on 10 mL of loading buffer supplemented with 100 mM sucrose in covered Petri dishes. Dishes were placed on an orbital shaker at 30 rpm to ensure aeration. At set time points of up to 48 hr, peels were removed and loaded with the viability stain fluorescein diacetate (5 μL of a 100 mM stock in acetone added to 10 mL of loading buffer) for 10 min, washed, and examined using an epifluorescence microscope (450- to 490-nm bandpass excitation filter, 515-nm longpass emission filter). Viability was scored for both guard cells and epidermal cells.

ACKNOWLEDGMENTS

We thank Drs. Pierre Ricci and Harald Keller for supplying us with cryptogein. We also thank Shlomit Bleichman for her excellent technical assistance and Drs. Hillel Fromm, Avihai Danon, Ron Mitler, and Carlos Gitler for helpful discussion and critical reading of the manuscript. This work was supported by a European Union Grant for Biotechnology and a grant from the Israeli Ministry of Science. A.C.A. was supported by a long-term EMBO postdoctoral fellowship. R.F. is a recipient of the Jack and Florence Goodman Career Development Chair.

Received March 24, 1997; accepted July 15, 1997.

REFERENCES

Agró, A.F., and Rossi, A. (1992). Copper-containing plant oxidases. Biochem. Soc. Trans. **20,** 369–373.

Angelini, R., Bragaloni, M., Federico, R., Infantino, A., and Porta-Puglia, A. (1993). Involvement of polyamines, diamine oxidase and peroxidase in resistance of chickpea to *Ascochyta rabiei*. J. Plant Physiol. **142,** 704–709.

Apostol, I., Heinstein, P.F., and Low, P.S. (1989). Rapid stimulation of an oxidative burst during elicitation of cultured plant cells. Plant Physiol. **90,** 109–116.

Bae, Y.S., Kang, S.W., Seo, M.S., Baines, I.C., Tekle, E., Chock, P.B., and Rhee, S.G. (1997). Epidermal growth factor (EGF)–induced generation of hydrogen peroxide. J. Biol. Chem. **272,** 217–221.

Baker, C.J., and Orlandi, E.W. (1995). Active oxygen in plant pathogenesis. Annu. Rev. Phytopathol. **33,** 299–321.

Baker, M.A., Cerniglia, G.J., and Zaman, A. (1990). Microtiter plate assay for the measurement of glutathione and glutathione disulfide in large numbers of biological samples. Anal. Biochem. **190,** 360–365.

Bi, Y.-M., Kenton, P., Mur, L., Darby, R., and Draper, J. (1995). Hydrogen peroxide does not function downstream of salicylic acid in the induction of PR protein expression. Plant J. **8,** 235–245.

Bottin, A., Véronési, D., Pontier, D., Esquerré-Tugayé, M.-T., Blein, J.-P., Rusterucci, C., and Ricci, P. (1994). Differential responses of tobacco cells to elicitors from two *Phytophthora* species. Plant Physiol. Biochem. **32,** 373–378.

Bowell, G.P., Butt, V.S., Davies, D.R., and Zimmerlin, A. (1995). The origin of the oxidative burst in plants. Free Radical Res. **23,** 517–532.

Cathcart, R., Schwiers, E., and Ames, B.N. (1983). Detection of picomole levels of hydroperoxides using a fluorescent dichlorofluorescein assay. Anal. Biochem. **134,** 111–116.

Chamnongpol, S., Willekens, H., Langebartels, C., Van Montagu, M., Inzé, D., and Van Camp, W. (1996). Transgenic tobacco with a reduced catalase activity develops necrotic lesions and induces pathogenesis-related expression under high light. Plant J. **10,** 491–503.

Chandra, S., Martin, G.B., and Low, P.S. (1996). The Pto kinase mediates a signaling pathway leading to the oxidative burst in tomato. Proc. Natl. Acad. Sci. USA **93,** 13393–13397.

Chen, Z., Silva, H., and Klessig, D.F. (1993). Active oxygen species in the induction of plant systemic acquired resistance by salicylic acid. Science **262,** 1883–1886.

Danon, A., and Mayfield, S.P. (1994). Light-regulated translation of chloroplast messenger RNAs through redox potential. Science **266,** 1717–1719.

Desikan, R., Hancock, J.T., Coffey, M.J., and Neill, S.J. (1996). Generation of active oxygen in elicited cells of *Arabidopsis thaliana* is mediated by a NADPH oxidase-like enzyme. FEBS Lett. **382,** 213–217.

Devary, Y., Gottlieb, R.A., Smeal, T., and Karin, M. (1992). The mammalian utraviolet response is triggered by activation of Src tyrosine kinases. Cell **71,** 1081–1091.

Dietrich, R.J., Richberg, M.H., Schmidt, R., Dean, C., and Dangl, J.L. (1997). A novel zinc finger protein is encoded by the Arabidopsis *LSD1* gene and functions as a negative regulator of plant cell death. Cell **88,** 685–694.

Doke, N., Miura, Y., Sanchez, L.M., Park, H.-J., Noritake, T., Yoshioka, H., and Kawakita, K. (1996). The oxidative burst protects plants against pathogen attack: Mechanism and role as an emergency signal for plant bio-defense—A review. Gene **179,** 45–51.

Doussiére, J., and Vignais, P.V. (1992). Diphenylene iodonium as an inhibitor of the NADPH oxidase complex of bovine neutrophils. Eur. J. Biochem. **208,** 61–71.

Durner, J., and Klessig, D.F. (1995). Inhibition of ascorbate peroxidase by salicylic acid and 2,6-dichloroisonicotinic acid, two inducers of plant defense responses. Proc. Natl. Acad. Sci. USA **92,** 11312–11316.

Foyer, C.H., Lelandais, M., and Kunert, K.J. (1994). Photoxidative stress in plants. Physiol. Plant. **92,** 696–717.

Green, R., and Fluhr, R. (1995). UV-B–induced PR-1 accumulation is mediated by active oxygen species. Plant Cell **7,** 203–212.

Groom, Q.J., Torres, M.A., Fordham-Skelton, A.P., Hammond-Kosack, K.E., and Jones, J.D.G. (1996). *RbohA*, a rice homologue of the mammalian *gp91phox* respiratory burst oxidase gene. Plant J. **10,** 515–522.

Håkansson, G., and Allen, J.F. (1995). Histidine and tyrosine phosphorylation in pea mitochondria: Evidence for protein phosphorylation in respiratory redox signaling. FEBS Lett. **372,** 238–242.

Hammond-Kosack, K.E., and Jones, J.D.G. (1996). Resistance gene–dependent plant defense responses. Plant Cell **8,** 1773–1791.

Hideg, É., and Vass, I. (1996). UV-B induced free radical production in plant leaves and isolated thylakoid membranes. Plant Sci. **115,** 251–260.

Hille, R., and Massey, V. (1985). Molybdenum-containing hydroxylases: Xanthine oxidase, aldehyde oxidase, and sulfite oxidase. In Molybdenum Enzymes, T.G. Spiro, ed (New York: John Wiley and Sons), pp. 443–517.

Huang, R.-P., Wu, J.-X., Fan, Y., and Adamson, E.D. (1996). UV activates growth factor receptors via reactive oxygen intermediates. J. Cell Biol. **133,** 211–220.

Inzé, D., and Van Montagu, M. (1995). Oxidative stress in plants. Curr. Opin. Biotechnol. **6,** 153–158.

Jabs, T., Dietrich, R.A., and Dangl, J.L. (1996). Initiation of runaway cell death in an *Arabidopsis* mutant by extracellular superoxide. Science **273,** 1853–1856.

Knox, P., and Dodge, A.D. (1984). Photodynamic damage to plant leaf tissue by rose bengal. Plant Sci. Lett. **37,** 3–7.

Levine, A., Tenhaken, R., Dixon, R., and Lamb, C. (1994). H_2O_2 from the oxidative burst orchestrates the plant hypersensitive disease resistance response. Cell **79,** 582–593.

Li, J., Ou-Lee, T.-M., Raba, R., Amundson, R.G., and Last, R.L. (1993). Arabidopsis flavonoid mutants are hypersensitive to UV-B irradiation. Plant Cell **5,** 171–179.

May, M.J., Hammond-Kosack, K.E., and Jones, J.D.G. (1996). Involvement of reactive oxygen species, glutathione metabolism, and lipid peroxidation in the *Cf*-gene–dependent defense response of tomato cotyledons induced by race-specific elicitors of *Cladosporium fulvum*. Plant Physiol. **110,** 1367–1379.

Mehdy, M.C. (1994). Active oxygen species in plant defense against pathogens. Plant Physiol. **105,** 467–472.

Meyer, M., Schreck, R., and Baeuerle, P.A. (1993). H_2O_2 and antioxidants have opposite effects on activation of NF-κB and AP-1 in intact cells: AP-1 as a secondary antioxidant-responsive factor. EMBO J. **12,** 2005–2015.

Milat, M.-L., Ricci, P., Bonnet, P., and Blein, J.-P. (1990). Capsidiol and ethylene production by tobacco cells in response to cryptogein, an elicitor from *Phytophthora cryptogea*. Phytochemistry **30,** 2171–2173.

Murphy, T.M., and Auh, C.-K. (1996). The superoxide synthases of plasma membrane preparations from cultured rose cells. Plant Physiol. **110,** 621–629.

Naton, B., Hahlbrock, K., and Schmelzer, E. (1996). Correlation of rapid cell death with metabolic changes in fungus-infected, cultured parsley cells. Plant Physiol. **112,** 433–444.

Neuenschwander, U., Vernooij, B., Friedrich, L., Uknes, S., Kessmann, H., and Ryals, J. (1995). Is hydrogen peroxide a second messenger of salicylic acid in systemic acquired resistance? Plant J. **8,** 227–233.

Ninnemann, H., and Maier, J. (1996). Indications for the occurrence of nitric-oxide synthases in fungi and plants and the involvement in photoconidiation of *Neurospora crassa*. Photochem. Photobiol. **64,** 393–398.

Ori, N., Eshed, Y., Pinto, P., Paran, I., Zamir, D., and Fluhr, R. (1997). TAO1—A representative of the molybdenum cofactor containing hydroxylases from tomato. J. Biol. Chem. **272,** 1019–1025.

Otte, O., and Barz, W. (1996). The elicitor-induced oxidative burst in cultured chickpea cells drives the rapid insolubilization of two cell wall structural proteins. Planta **200,** 238–246.

Rao, K.M., Padmanabhan, J., Kilby, D.L., Cohen, H.J., Currie, M.S., and Weinberg, J.B. (1992). Flow cytometric analysis of nitric oxide production in human neutrophils using dichlorofluorescein diacetate in the presence of a calmodulin inhibitor. J. Leukocyte Biol. **51,** 496–500.

Rao, M.V., Paliyath, G., and Ormrod, D.P. (1996). Ultraviolet-B- and ozone-induced biochemical changes in antioxidant ezymes of *Arabidopsis thaliana*. Plant Physiol. **110,** 125–136.

Ricci, P., Bonnet, P., Huet, J.-C., Sallantin, M., Beauvais-Cante, F., Bruneteau, M., Billard, V., Michel, G., and Pernollet, J.-C. (1989). Structure and activity of proteins from pathogenic fungi *Phytophthora* eliciting necrosis and acquired resistance in tobacco. Eur. J. Biochem. **183,** 555–563.

Salzer, P., Hebe, G., Reith, A., Zitterell-Haid, B., Stransky, H., Gaschler, K., and Hager, A. (1996). Rapid reactions of spruce cells to elicitors released from the ectomycorrhizal fungus *Hebeloma crustuliniforme*, and inactivation of these elicitors by extracellular spruce enzymes. Planta **198,** 118–126.

Schreck, R., Albermann, K., and Bauerle, P.A. (1992). Nuclear factor κB: An oxidative stress-responsive transcription factor of eukaryotic cells (a review). Free Radical Res. Commun. **17,** 221–237.

Schwacke, R., and Hager, A. (1992). Fungal elicitors induce a transient release of active oxygen species from cultured spruce cells that is dependent on Ca^{2+} and protein kinase activity. Planta **187,** 136–141.

Scofield, S.R., Tobias, C.M., Rathjen, J.P., Chang, J.H., Lavelle, D.T., Michelmore, R.W., and Staskawicz, B.J. (1996). Molecular basis for gene-for-gene specificity in bacterial speck disease of tomato. Science **274,** 2063–2065.

Segal, A.W., and Abo, A. (1993). The biochemical basis of the NADPH oxidase of phagocytes. Trends Biochem. Sci. **18,** 43–47.

Sen, C.K., and Packer, L. (1996). Antioxidant and redox regulation of gene transcription. FASEB J. **10,** 709–720.

Sutherland, M.W. (1991). The generation of oxygen radicals during host plant responses to infection. Physiol. Mol. Plant Pathol. **39,** 79–93.

Tang, X., Frederick, R.D., Zhou, J., Halterman, D.A., Jia, Y., and Martin, G.B. (1996). Initiation of plant disease resistance by physical interaction of AvrPto and Pto kinase. Science **274,** 2060–2063.

Tavernier, E., Wendehenne, D., Blein, J.-P., and Pugin, A. (1995). Involvement of free calcium in action of cryptogein, a proteinaceous elicitor of hypersensitive reaction in tobacco cells. Plant Physiol. **109,** 1025–1031.

Tipping, A.J., and McPherson, M.J. (1995). Cloning and molecular analysis of the pea seedling copper amine oxidase. J. Biol. Chem. **270,** 16939–16946.

Vera-Estrella, R., Blumwald, E., and Higgins, V.J. (1992). Effect of specific elicitors of *Cladosporium fulvum* on tomato suspension cells. Plant Physiol. **99,** 1208–1215.

Viard, M.-P., Martin, F., Pugin, A., Ricci, P., and Blein, J.-P. (1994). Protein phosphorylation is induced in tobacco cells by the elicitor cryptogein. Plant Physiol. **104,** 1245–1249.

Vowells, S.J., Sekhsaria, S., Malech, H.L., Shalit, M., and Fleisher, T.A. (1995). Flow cytometric analysis of the granulocyte respiratory burst: A comparison study of fluorescent probes. J. Immunol. Methods **178,** 89–97.

Wu, X., Bishopric, N.H., Discher, D.J., Murphy, B.J., and Webster, K.A. (1996). Physical and functional sensitivity of zinc finger transcription factors to redox change. Mol. Cell. Biol. **16,** 1035–1046.

Yahraus, T., Chandra, S., Legendre, L., and Low, P.S. (1995). Evidence for a mechanically induced oxidative burst. Plant Physiol. **109,** 1259–1266.

Yang, Y., and Klessig, D.F. (1996). Isolation and characterization of a tobacco mosaic virus–inducible *myb* oncogene homolog from tobacco. Proc. Natl. Acad. Sci. USA **93,** 14972–14977.